NOTE: THE FIGURES IN THIS SECTION ARE INTENDED TO SHOW THE REPRESENTATIVE DATA.
THEY ARE NOT MEANT TO BE COMPLETE COMPILATIONS OF ALL THE WORLD'S RELIABLE DATA.

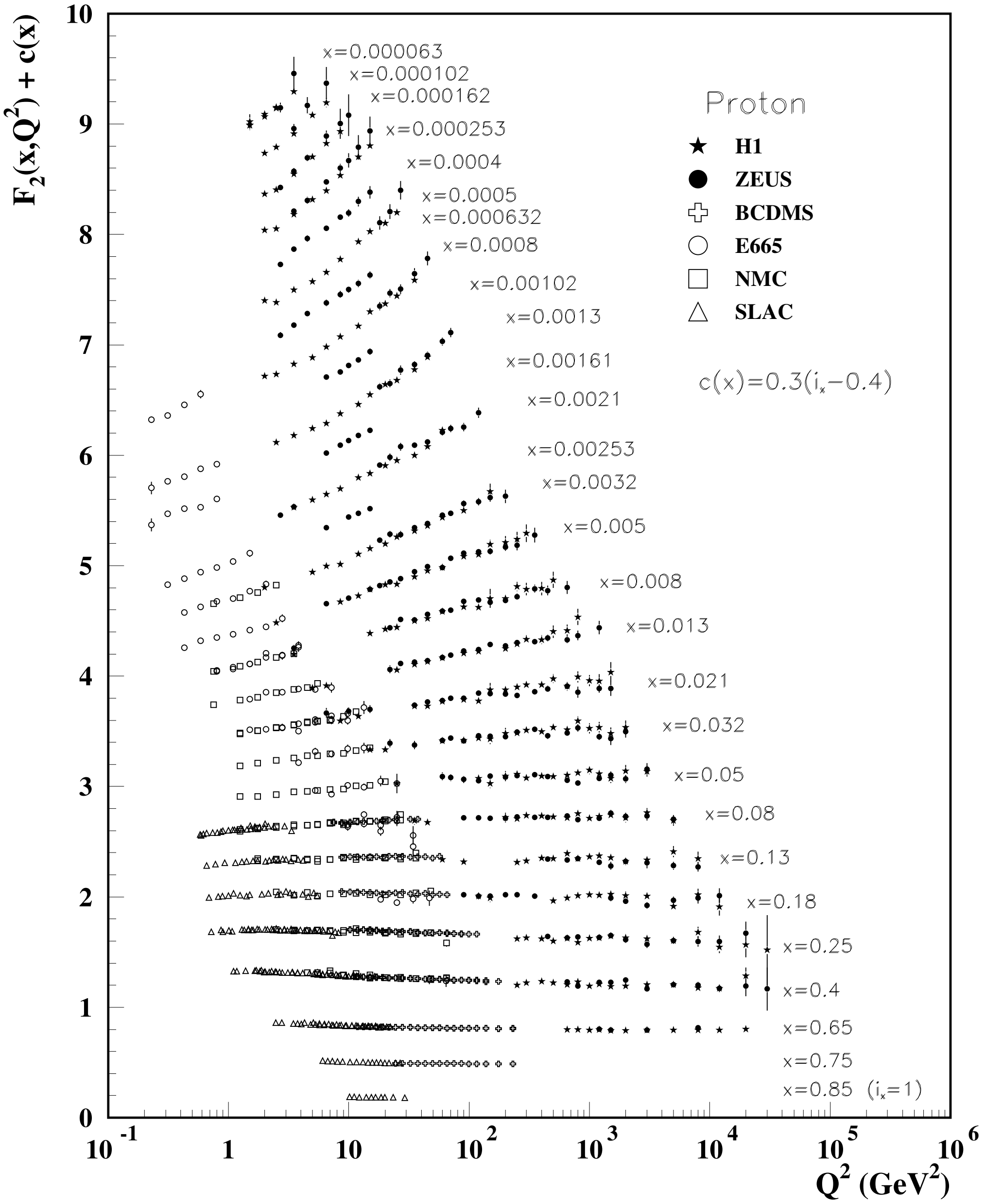

Figure 14.6: The proton structure function F_2^p measured in electromagnetic scattering of positrons on protons (collider experiments ZEUS and H1), in the kinematic domain of the HERA data, for $x > 0.00006$ (*cf.* Fig. 14.9 for data at smaller x and Q^2), and for electrons (SLAC) and muons (BCDMS, E665, NMC) on a fixed target. Statistical and systematic errors added in quadrature are shown. The data are plotted as a function of Q^2 in bins of fixed x. The ZEUS binning in x is used in this plot; all other data are rebinned to the x values of the ZEUS data. For the purpose of plotting, a constant $c(x) = 0.3(i_x - 0.4)$ is added to F_2^p, where i_x is the number of the x bin ranging from $i_x = 1$ ($x = 0.85$) to $i_x = 28$ ($x = 0.000063$). References: **H1**— C. Adloff *et al.*, Eur. Phys. J. **C21**, 33 (2001); C. Adloff *et al.*, Eur. Phys. J. **C13**, 609 (2000); **ZEUS**—S. Chekanov *et al.*, Eur. Phys. J. **C21**, 443 (2001); **BCDMS**—A.C. Benvenuti *et al.*, Phys. Lett. **B223**, 485 (1989) (as given in [46]); **E665**—M.R. Adams *et al.*, Phys. Rev. **D54**, 3006 (1996); **NMC**—M. Arneodo *et al.*, Nucl. Phys. **B483**, 3 (97); **SLAC**—L.W. Whitlow *et al.*, Phys. Lett. **B282**, 475 (1992).

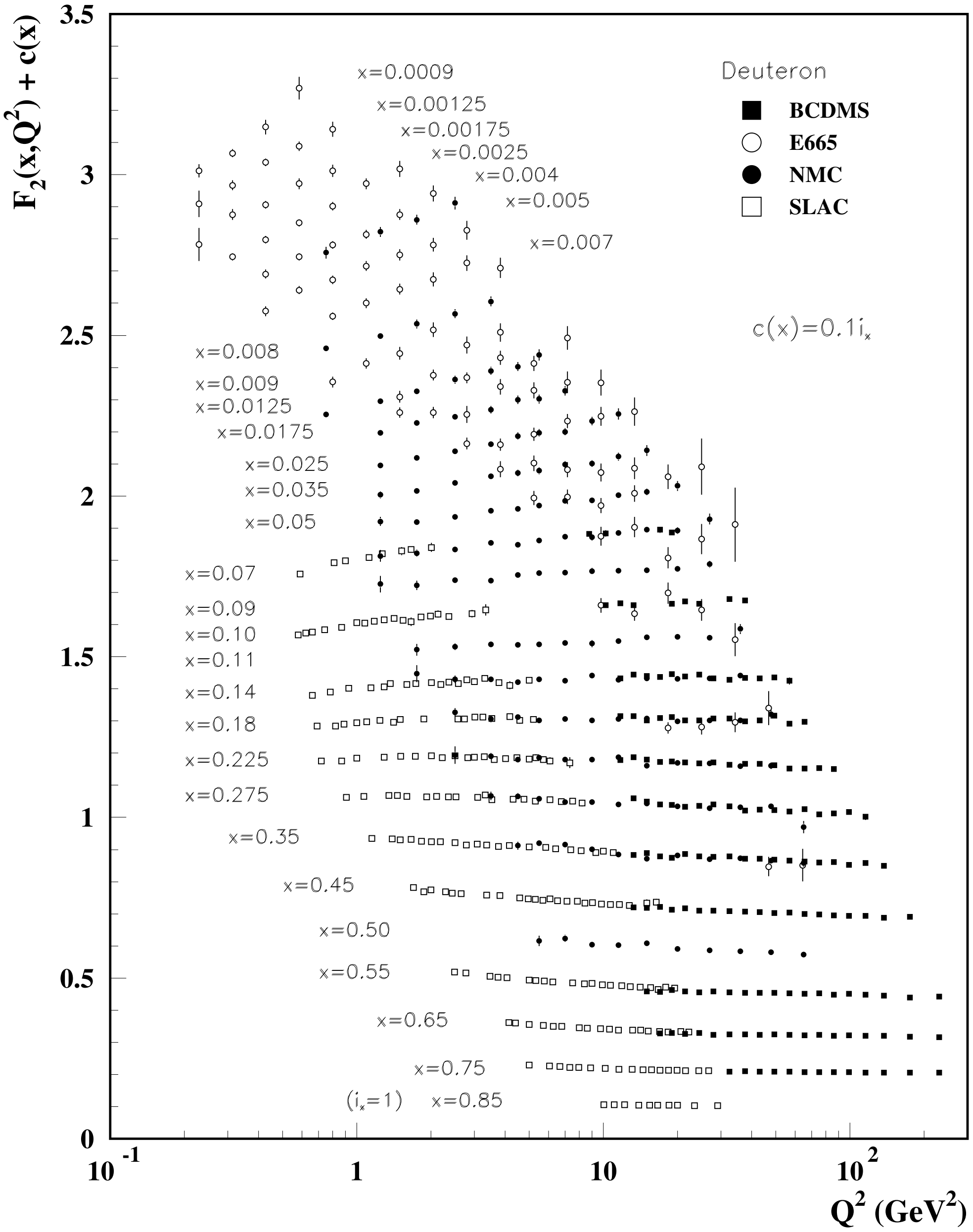

Figure 14.7: The deuteron structure function F_2^d measured in electromagnetic scattering of electrons (SLAC) and muons (BCDMS, E665, NMC) on a fixed target, shown as a function of Q^2 for bins of fixed x. Statistical and systematic errors added in quadrature are shown. For the purpose of plotting, a constant $c(x) = 0.1 i_x$ is added to F_2^p where i_x is the number of the x bin, ranging from 1 ($x = 0.85$) to 29 ($x = 0.0009$). References: **BCDMS**—A.C. Benvenuti *et al.*, Phys. Lett. **B237**, 592 (1990). **E665, NMC, SLAC**—same references as Fig. 14.6.

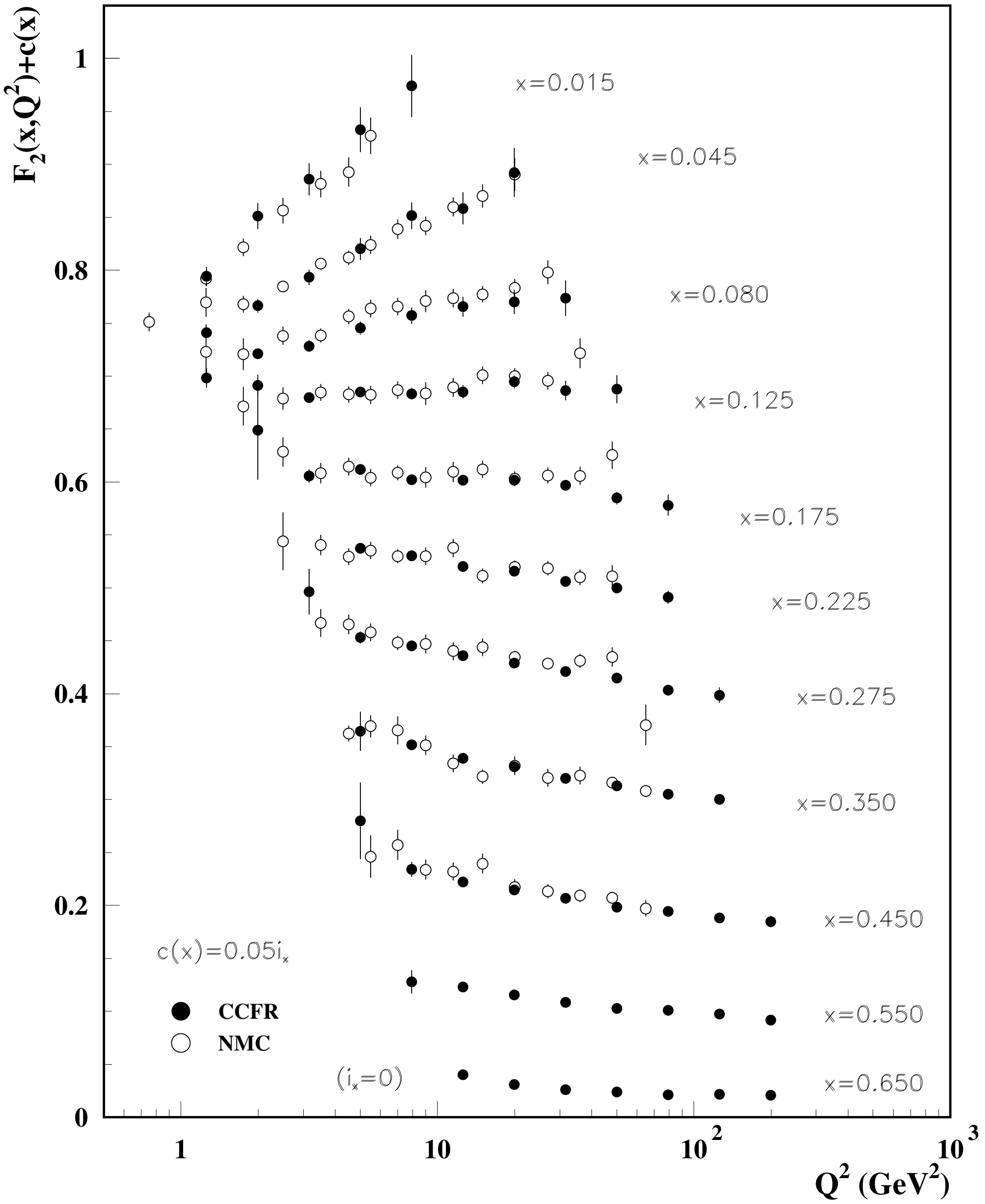

Figure 14.8: The deuteron structure function F_2 measured in deep inelastic scattering of muons on a fixed target (NMC) is compared to the structure function F_2 from neutrino-iron scattering (CCFR) using $F_2^{\mu} = (5/18)F_2^{\nu} - x(s+\overline{s})/6$, where heavy target effects have been taken into account. The data are shown versus Q^2, for bins of fixed x. The NMC data have been rebinned to CCFR x values. Statistical and systematic errors added in quadrature are shown. For the purpose of plotting, a constant $c(x) = 0.05i_x$ is added to F_2 where i_x is the number of the x bin, ranging from 0 ($x = 0.65$) to 10 ($x = 0.015$). References: **NMC**—M. Arneodo *et al.*, Nucl. Phys. **B483**, 3 (97); **CCFR/NuTeV**—U.K. Yang *et al.*, Phys. Rev. Lett. **86**, 2741 (2001).

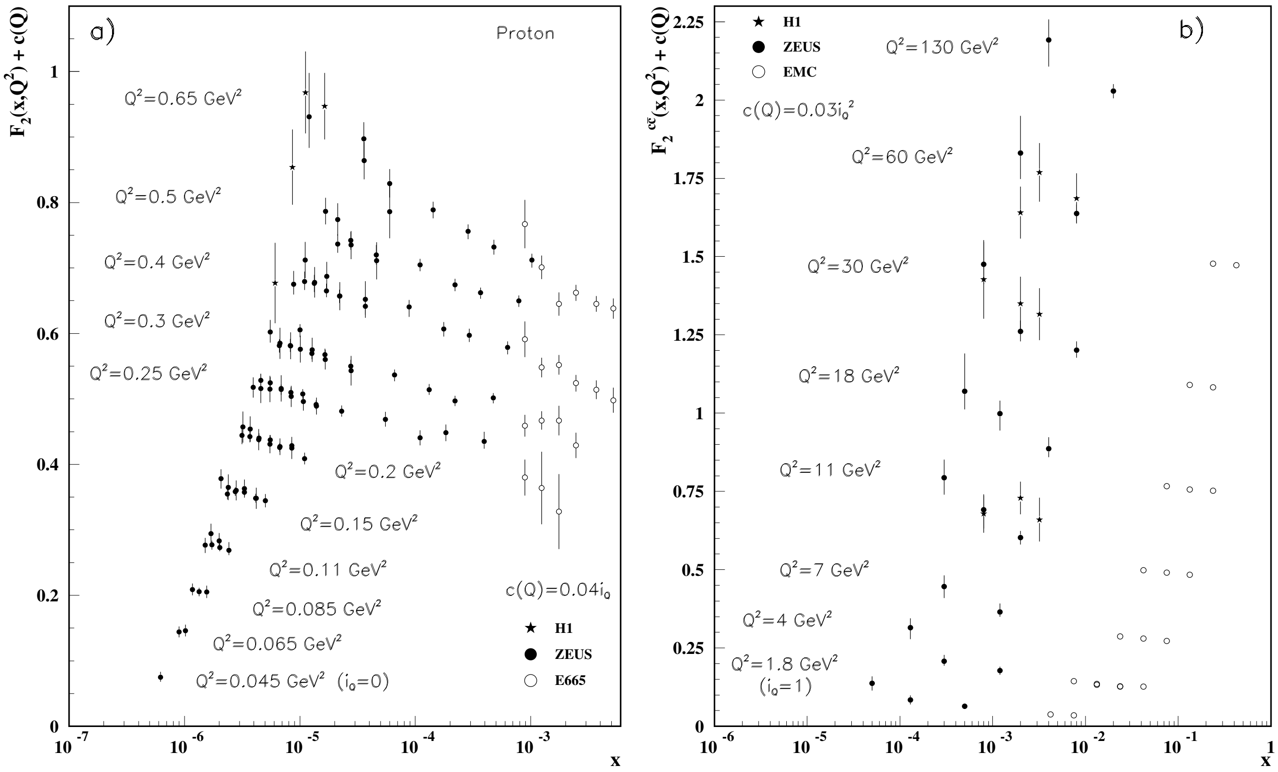

Figure 14.9: a) The proton structure function F_2^p at small x and Q^2, measured in electromagnetic scattering of positrons (H1, ZEUS) and muons (E665) on protons. For the purpose of plotting, a constant $c(Q) = 0.04 i_Q$ is added to F_2^p where i_Q is the number of the Q^2 bin, ranging from 0 ($Q^2 = 0.045$ GeV^2) to 10 ($Q^2 = 0.65$ GeV^2). References: **ZEUS**—J. Breitweg *et al.*, Phys. Lett. **B407**, 432 (1997); J. Breitweg *et al.*, Phys. Lett. **B487**, 53 (2000); J. Breitweg *et al.*, Eur. Phys. J. **C7**, 609 (1999); **H1**—C. Adloff *et al.*, Nucl. Phys. **B497**, 3 (1997); **E665**—M.R. Adams *et al.*, Phys. Rev. **D54**, 3006 (1996).

b) The charm structure function $F_2^{c\bar{c}}(x)$, i.e. that part of the inclusive structure function F_2^p arising from the production of charm quarks, measured in electromagnetic scattering of positrons on protons (H1, ZEUS) and muons on iron (EMC). For the purpose of plotting, a constant $c(Q) = 0.03 i_Q^2$ is added to $F_2^{c\bar{c}}$ where i_Q is the number of the Q^2 bin, ranging from 1 ($Q^2 = 1.8$ GeV^2) to 8 ($Q^2 = 130$ GeV^2). References: **ZEUS**—J. Breitweg *et al.*, Eur. Phys. J. **C12**, 35 (2000); **H1**—C. Adloff *et al.*, Z. Phys. **C72**, 593 (1996); **EMC**—J.J. Aubert *et al.*, Nucl. Phys. **B213**, 31 (1983).

Statistical and systematic errors added in quadrature are shown for both plots. The data are given as a function of x in bins of Q^2.

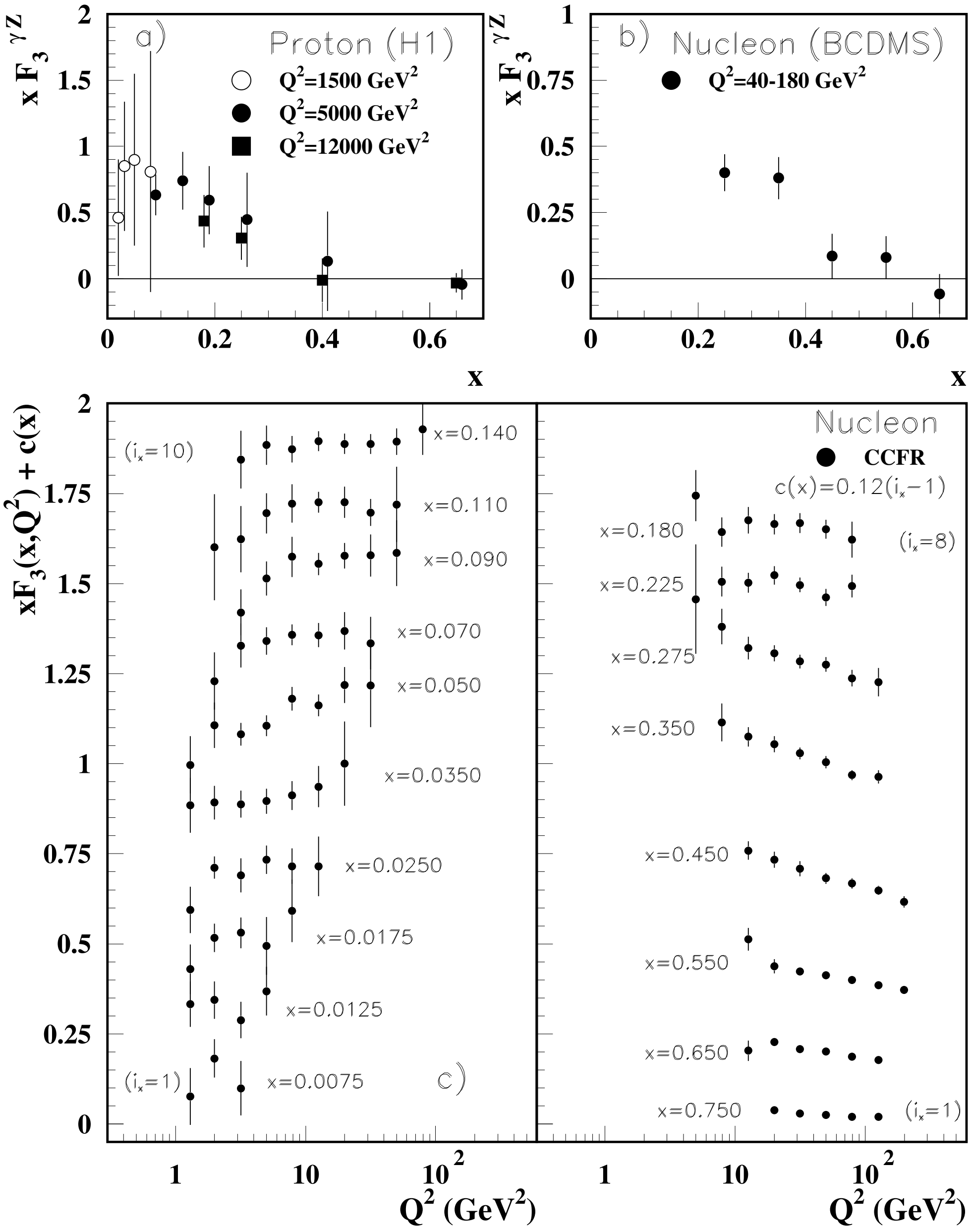

Figure 14.10: The structure function $xF_3^{\gamma Z}$ measured in electroweak scattering of **a)** electrons on protons (H1) and **b)** muons on carbon (BCDMS). Statistical and systematic errors added in quadrature are shown. References: **H1**—C. Adloff *et al.*, Eur. Phys. J. **C19**, 269 (2001); **BCDMS**—A. Argento *et al.*, Phys. Lett. **B140**, 142 (1984).

c) The structure function xF_3 of the nucleon measured in ν-Fe scattering. Statistical and systematic errors added in quadrature are shown. The data are plotted as a function of Q^2 in bins of fixed x. For the purpose of plotting, a constant $c(x) = 0.12(i_x - 1)$ is added to xF_3, where i_x is the number of the x bin as shown in the plot. References: **CCFR**–W. G. Seligman *et al.*, Phys. Rev. Lett. **79**, 1213 (1997).

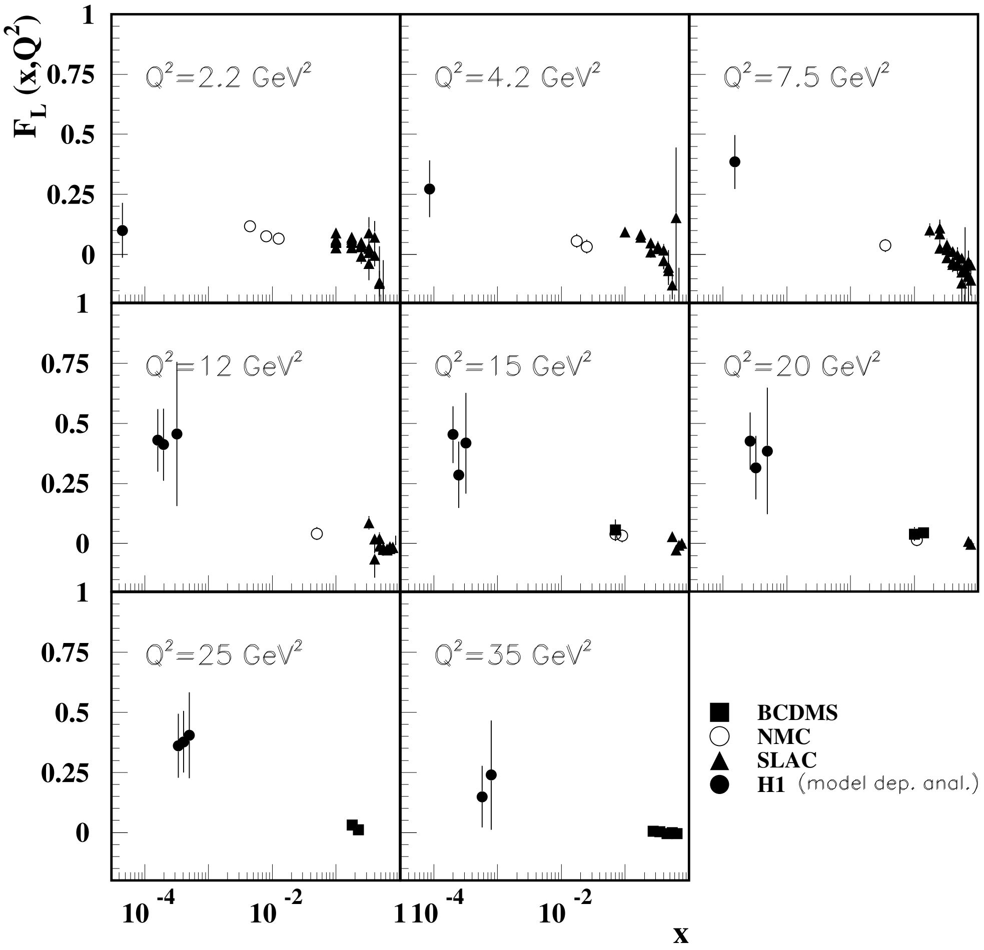

Figure 14.11: The longitudinal structure function F_L as a function of x in bins of fixed Q^2 measured on the proton (except for the SLAC data which also contain deuterium data). The H1 result requires the assumption of the validity of the QCD form for the F_2 structure function in order to extract F_L. BCDMS, NMC, and SLAC results are from measurements of R (the ratio of longitudinal to transverse photon absorption cross sections) which are converted to F_L by using the BDCMS parameterization of F_2 (A.C. Benvenuti *et al.*, Phys. Lett. **B223**, 485 (1989)). It is assumed that the Q^2 dependence of the fix-target data is small within a given Q^2 bin. Statistical and systematic errors added in quadrature are shown. References: **H1**—C. Adloff *et al.*, Eur. Phys. J. **C21**, 33 (2001); **BCDMS**—A. Benvenuti *et al.*, Phys. Lett. **B223**, 485 (1989); **NMC**—M. Arneodo *et al.*, Nucl. Phys. **B483**, 3 (1997); **SLAC**— L.W. Whitlow *et al.*, Phys. Lett. **B250**, 193 (1990) and numerical values from the thesis of L.W. Whitlow (SLAC-357).

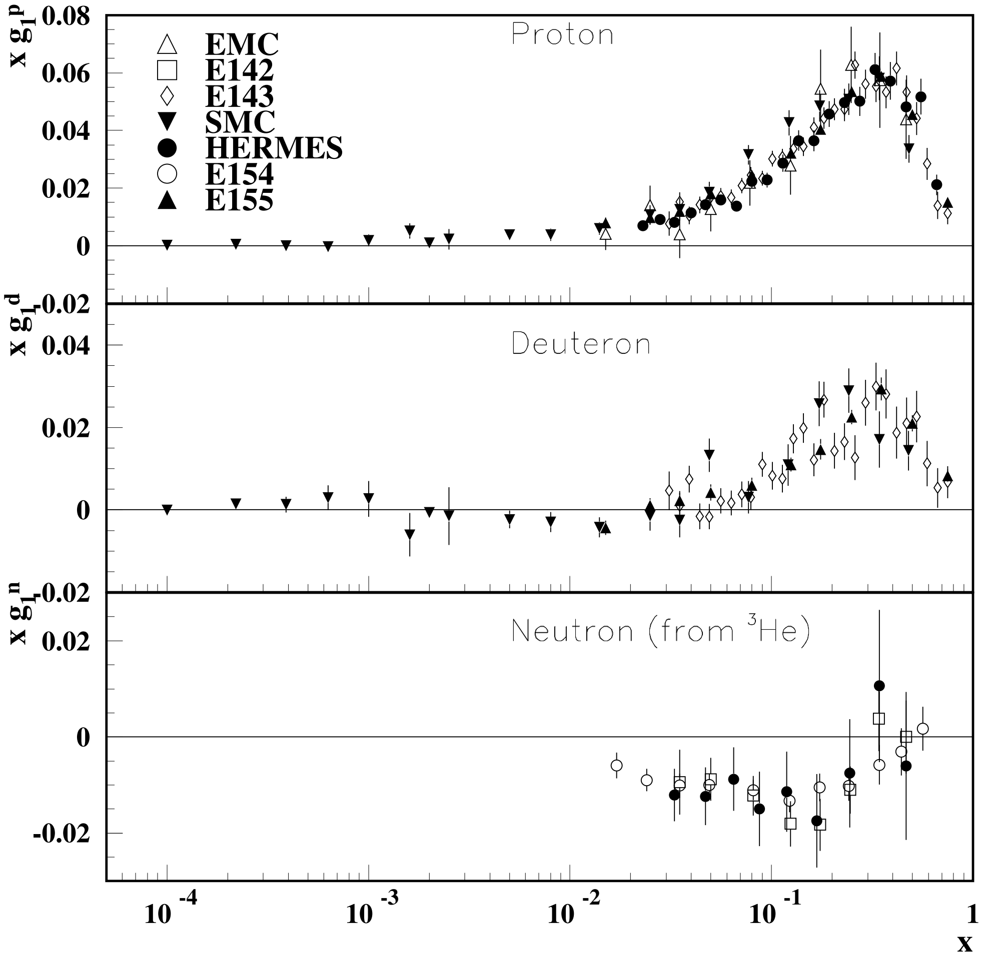

Figure 14.12: The spin-dependent structure function $xg_1(x)$ of the proton, deuteron, and neutron (from ^{3}He target) measured in deep inelastic scattering of polarized electrons/positrons: E142 ($Q^2 \sim 0.3 - 10$ GeV^2), E143 ($Q^2 \sim 0.3 - 10$ GeV^2), E154 ($Q^2 \sim 1 - 17$ GeV^2), E155 ($Q^2 \sim 1 - 40$ GeV^2), HERMES ($Q^2 \sim 0.8 - 20$ GeV^2) and muons: EMC ($Q^2 \sim 1.5 - 100$ GeV^2), SMC ($Q^2 \sim 0.01 - 100$ GeV^2), shown at the measured Q^2 (except for EMC data given $Q^2 = 10.7$ GeV^2 and E155 data given at $Q^2 = 5$ GeV^2). Note that $g_1^n(x)$ may also be extracted by taking the difference between $g_1^d(x)$ and $g_1^p(x)$, but these values have been omitted in the bottom plot for clarity. Statistical and systematic errors added in quadrature are shown. References: **EMC**—J. Ashman *et al.*, Nucl. Phys. **B328**, 1 (1989); **E142**—P.L. Anthony *et al.*, Phys. Rev. **D54**, 6620 (1996); **E143**—K. Abe *et al.*, Phys. Rev. **D58**, 112003 (1998); **SMC**—B. Adeva *et al.*, Phys. Rev. **D58**, 112001 (1998), B. Adeva *et al.*, Phys. Rev. **D60**, 072004 (1999) and Erratum-Phys. Rev. **D62**, 079902 (2000); **HERMES**—A. Airapetian *et al.*, Phys. Lett. **B442**, 484 (1998) and K. Ackerstaff *et al.*, Phys. Lett. **B404**, 383 (1997); **E154**—K. Abe *et al.*, Phys. Rev. Lett. **79**, 26 (1997); **E155**—P.L. Anthony *et al.*, Phys. Lett. **B463**, 339 (1999) and P.L. Anthony *et al.*, Phys. Lett. **B493**, 19 (2000).